

# Dynamics of a quantum two-state system in a linearly driven quantum bath

J. Reichert,<sup>1,2</sup> P. Nalbach,<sup>3</sup> and M. Thorwart<sup>1,2</sup>

<sup>1</sup>*I. Institut für Theoretische Physik, Universität Hamburg, Jungiusstraße 9, 20355 Hamburg, Germany*

<sup>2</sup>*The Hamburg Centre for Ultrafast Imaging, Luruper Chaussee 149, 22761 Hamburg, Germany*

<sup>3</sup>*Westfälische Hochschule, Münsterstraße 265, 46397 Bocholt, Germany*

(Dated: September 30, 2016)

When an open quantum system is driven by an external time-dependent force, the coupling of the driving to the central system is usually included whereas the impact of the driving field on the bath is neglected. We investigate the effect of a quantum bath of linearly driven harmonic oscillators on the relaxation dynamics of a quantum two-level system which itself is not directly driven. In particular, we calculate the frequency-dependent response of the system when the bath is subject to a Dirac and a Gaussian driving-pulse. We show that a time-retarded effective force on the system is induced by the driven bath which depends on the full history of the perturbation and the spectral characteristics of the underlying bath. In particular, when a structured Ohmic bath with a pronounced Lorentzian peak is considered, the dynamical response of the system to a driven bath is qualitatively different as compared to the undriven bath. Specifically, additional resonances appear which can be directly associated to a Jaynes-Cummings-like effective energy spectrum.

## I. INTRODUCTION

The effect of environmental fluctuations on the dynamics of quantum systems has been a longstanding focus of quantum statistical physics. Indeed, the modern fields of quantum dissipation and open quantum systems treat a physical problem by separating it into an identifiable “system”, which encompasses a few controllable degrees of freedom, and an environmental “bath” (or reservoir) [1], which consists of infinitely many degrees of freedom and exerts fluctuating forces on the central system. In many physical situations, the spectral statistics of the (classical or quantum) fluctuations is Gaussian, such that the underlying physical model of a harmonic bath is adequate. Thereby, infinitely many harmonic oscillators are used in conjunction with a bi-linear system-bath coupling. After integrating over the harmonic bath degrees of freedom, a reduced density operator of the system is constructed whose effective non-unitary time-dependence is studied.

A minimal model system which allows to study the role of dissipative fluctuations on the transition dynamics between two quantum mechanical states is the spin-boson model. It describes a quantum two-level system (TLS) coupled to a bath of harmonic oscillators [2] and has been used for the analysis of such diverse physical phenomena as tunneling of defects in low-temperature amorphous materials [3–6], the role of the solvent on electron transfer in chemical reactions [7], energy transfer in biomolecular photoactive complexes [8], or the analysis of decoherence and relaxation properties of solid-state qubit devices realized in single-charge and spin quantum dots [9] and superconducting quantum interference devices [10].

A useful tool to investigate quantum systems is through application of a time-dependent external field [1, 11–13]. The impact of such time-dependent driving is usually included by way of a direct coupling of the external field to the central system of interest, while the impact of the time-dependent driving on the environment

is not included. It was recently realized, however, that ancillary driving of the reservoir itself is unavoidable in principle on the nanoscale in many physical applications [14]. In fact, as it was recently shown for two model systems, the system of interest becomes subject to an additional bath-induced force component, if an external time-dependent drive couples to the bath as well. For instance, the exact solution of the polarizability of a test molecule immersed in water which is also subject to external driving, reveals [14] that the frequency-dependent response is increased by about 30% as compared to the case when bath-driving is not considered. Moreover, the frequency-dependent response of a semiconducting nanocrystal placed in the vicinity of a metallic nanoparticle and both immersed in a solvent, was shown to be qualitatively altered when bath-driving is included [14]. Furthermore, the impact of coupling external driving to the environmental modes of driven superconducting tunnel junctions was shown to yield significant contributions [15, 16].

In this work, we study the way in which time-dependent driving of the harmonic modes of a quantum bath affects the relaxation dynamics of a quantum two-level system. This constitutes a generalization of the spin-boson model in which an external time-dependent driving force is coupled linearly to the bath. For simplicity, we do not consider an additional direct coupling of the external time-dependent force to the system itself, but focus our attention on the impact of the driven bath. We show explicitly that the driven bath generates a time-retarded effective force which acts on the two-level system. We address the relaxation dynamics in the regime of weak system-bath coupling such that the effective dynamics of the central quantum system can be described in terms of a quantum master equation with time-dependent rate coefficients. Specifically, we apply a suitable adiabatic Born-Markov approximation [1, 17–20] which is valid for not too fast driving. We consider two types of bath spectral densities, the simple structureless

Ohmic bath and a structured Ohmic bath which contains a single pronounced harmonic mode. The latter is known to be equivalent to a cavity QED setup [21]. We calculate the response of the dissipative quantum two-level system to time-dependent bath-driving with a  $\delta$ -shaped as well as a Gaussian-shaped driving pulse. The effective bath-induced force is given in exact form. We show that the response of the two-level system to the driven bath is noticeably altered. For the unstructured Ohmic bath, the resonant response of the quantum two-level system decreases in a driven bath as compared to the undriven case. A qualitatively different response arises when the structured Ohmic bath is driven. Additional resonant peaks appear in the response of the system when the external drive matches resonances related to environmental modes. The present formulation within the general context of quantum dissipation could potentially open up novel pathways to control the dynamics of quantum two-level systems by manipulating their environment through time-dependent control fields.

## II. MODEL HAMILTONIAN

We consider a model of a quantum mechanical two-level system which is coupled to a linearly driven quantum bath. The associated total time-dependent Hamiltonian

$$H(t) = H_S + H_{SB} + H_B + H_{IB}(t) \quad (1)$$

is the sum of a system Hamiltonian  $H_S$  and a bath Hamiltonian  $H_B$ , along with a part  $H_{SB}$  that describes the system-bath coupling. The new term  $H_{IB}(t)$  represents the effect of external time-dependent driving on the bath.

To be specific, we consider in this work a symmetric quantum mechanical two-state system ( $\hbar = 1$  and  $\sigma_{i=x,z}$  denote the Pauli matrices) with

$$H_S = \frac{\Delta}{2} \sigma_x, \quad (2)$$

which couples to a bath of harmonic oscillators

$$H_B = \sum_j^N \omega_j \left( b_j^\dagger b_j + \frac{1}{2} \right), \quad (3)$$

via

$$H_{SB} = -\frac{\sigma_z}{2} \sum_j^N c_j \left( b_j + b_j^\dagger \right) \quad (4)$$

with coupling constants  $c_j$ . Here,  $b_j$  and  $b_j^\dagger$  denote the corresponding annihilation and creation operators of the  $j$ -th bath mode. The new term describes the coupling of the bath to an external, classical force  $F(t)$  and is included as

$$H_{IB}(t) = -\frac{F(t)}{2} \sum_j^N d_j \left( b_j + b_j^\dagger \right), \quad (5)$$

where the  $d_j$  denote the associated coupling constants. The driving of each bath mode is assumed to be of dipolar type, coupling to the displacement of the oscillators. This linear (or additive) form of the coupling does not modify the mean square displacements of the oscillators and, thus, does not alter the (equilibrium) temperature of the bath which is fixed at the initial time (see below). This would be different if the external force coupled parametrically, i.e.,  $H_{IB}^{\text{para}}(t) = -\frac{F(t)}{2} \sum_j^N d_j b_j^\dagger b_j$ .

As usual [1], we characterize the bath by the spectral density

$$J(\omega) = \pi \sum_j^N c_j^2 \delta(\omega - \omega_j), \quad (6)$$

with specific forms of  $J(\omega)$  given below.

The time dependence of the bath Hamiltonian requires some attention in view of the initial condition for the dissipative dynamics. The most convenient choice is factorizing initial conditions. In this case, the system is assumed to be initially decoupled from the bath and the coupling is switched on instantaneously at time  $t_0$  [1]. For the time-dependent bath-driving of Eq. (5), we consider pulse-shaped driving, in particular a  $\delta$ -shaped and a Gaussian pulse, starting at time  $t_a$ . Figure 1 shows the scheme which we follow throughout this work. We assume the bath to be in thermal equilibrium until time  $t_a$ . Then, the density matrix of the bath is given by  $\rho_B(t_a) = \rho_B^{\text{eq}} = e^{-\beta H_B} / \mathcal{Z}$  at the given temperature  $T = 1/\beta$  with  $k_B = 1$  ( $\mathcal{Z}$  is the equilibrium partition of the decoupled bath). At  $t = t_a$ , the action of the pulse on the bath is turned on and the interaction  $F(t)$  in Eq. (5) becomes nonzero. Subsequently, the bath evolves under the combined time evolution operator defined by

$$H_B^{\text{eff}}(t) = H_B + H_{IB}(t). \quad (7)$$

In addition, we consider the system-bath coupling  $H_{SB}$  to be active for times  $t > t_0$  onwards.

## III. DRIVEN BATH DYNAMICS

Due to the additivity of the external driving, it is convenient to address the Heisenberg operators  $b_j(t)$  of the bath. Therefore, we consider the time evolution of each bath operator  $b_j$  under the driven bath Hamiltonian of Eq. (7). The Heisenberg operators  $\tilde{b}_j(t)$  are found to be of the form [22]

$$\tilde{b}_j(t) = \tilde{b}_j^0(t) + \frac{1}{2} K_j(t, t_a) \quad (8)$$

with the Heisenberg operator under force-free time evolution

$$\tilde{b}_j^0(t) = b_j e^{-i\omega_j t}, \quad (9)$$

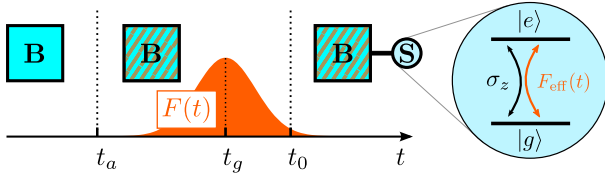


FIG. 1. General setup of a pulse-shaped bath drive. The bath (B) is in equilibrium until time  $t_a$ , when the bath driving force  $F(t)$  (orange and shown as a generic Gaussian pulse) is activated. Subsequently, the bath is driven (orange stripes), with the perturbation centered at some time  $t_g$ . At time  $t_0$  the system (S) is coupled to the driven bath. We consider a two-level system with the ground (g) and excited state (e) coupled to the harmonic bath. Bath driving leads to an additional effective force  $F_{\text{eff}}(t)$ , as shown in this work.

and the driving-induced term

$$K_j(t, t_a) = i \int_{t_a}^t dt' e^{i\omega_j(t'-t)} d_j F(t'). \quad (10)$$

The corresponding equation for  $\tilde{b}_j^\dagger(t)$  can be obtained by standard Hermitian conjugation.

### A. Effective force

Since each bath oscillator is not statically displaced, it follows that  $\tilde{b}_j^0(t)$  has zero average at equilibrium, i.e.,  $\langle \tilde{b}_j^0(t) \rangle_{\text{B}}^{\text{eq}} = 0$ . However, due to Eq. (10), linear bath driving induces a nonzero contribution, such that  $\langle \tilde{b}_j(t) \rangle_{\text{B}}^{\text{eq}} = K_j(t, t_a)/2$ . This implies

$$\begin{aligned} \langle H_{\text{SB}} \rangle_{\text{B}}(t) &= -\frac{\sigma_z}{2} \sum_j^N c_j \langle \tilde{x}_j(t) \rangle_{\text{B}}^{\text{eq}} \\ &= -\frac{\sigma_z}{2} \text{Re} \left[ \sum_j^N c_j K_j(t, t_a) \right] \equiv \frac{\sigma_z}{2} F_{\text{eff}}(t), \end{aligned} \quad (11)$$

where we inserted the dimensionless (Heisenberg) position operator  $\tilde{x}_j(t) = \tilde{b}_j(t) + \tilde{b}_j^\dagger(t)$ . This defines the effective force  $F_{\text{eff}}(t)$  which can be formulated in a convenient way by introducing an additional spectral density

$$\bar{J}(\omega) = \pi \sum_j^N d_j c_j \delta(\omega - \omega_j). \quad (12)$$

It incorporates the system-bath coupling constants  $c_j$  as well as the coupling constants of the external driving to the bath  $d_j$ . With this, the continuum limit of an infinitely dense spectrum of environmental modes can be performed. Then, the effective force follows as

$$F_{\text{eff}}(t) = \text{Im} \left[ \frac{1}{\pi} \int_0^\infty d\omega \bar{J}(\omega) \int_{t_a}^t dt' F(t') e^{i\omega(t'-t)} \right]. \quad (13)$$

It should be emphasized that the effective force is time-dependent and only nonzero for times  $t > t_0$  as it depends on the system-bath couplings  $c_j$ .

### B. Fluctuations

As the driving-induced term in Eq. (10) is proportional to the identity operator, a simple shift of the Heisenberg operator  $\tilde{b}_j(t)$  by the average  $\langle \tilde{b}_j(t) \rangle_{\text{B}}^{\text{eq}}$  allows us to recover an effective undriven time evolution. Accordingly, the shifted (Heisenberg) position operator fulfills  $\tilde{x}_j^{\text{eff}}(t) = \tilde{x}_j(t) - \langle \tilde{x}_j(t) \rangle_{\text{B}}^{\text{eq}} = \tilde{x}_j^0(t)$ . Consequently, the bath autocorrelation function  $\tilde{B}_{\text{C}}(t, s)$  and the bath response function  $B_{\text{R}}(t, s)$  remain unchanged compared to their equilibrium form. In particular, we have that

$$\begin{aligned} B_{\text{C}}(t, s) &= \left\langle \sum_{j, j'}^N \frac{c_j c_{j'}}{2} \{ \tilde{x}_j^{\text{eff}}(t), \tilde{x}_{j'}^{\text{eff}}(s) \} \right\rangle_{\text{B}}^{\text{eq}} \\ &= \sum_j^N c_j^2 \coth \left( \frac{\beta \hbar \omega_j}{2} \right) \cos(\omega_j(t-s)), \end{aligned} \quad (14)$$

$$\begin{aligned} B_{\text{R}}(t, s) &= \left\langle \sum_{j, j'}^N \frac{c_j c_{j'}}{2} i [ \tilde{x}_j^{\text{eff}}(t), \tilde{x}_{j'}^{\text{eff}}(s) ] \right\rangle_{\text{B}}^{\text{eq}} \\ &= \sum_j^N c_j^2 \sin(\omega_j(t-s)), \end{aligned} \quad (15)$$

where we use  $\{ \cdot, \cdot \}$  to denote the anticommutator. These averages over system-bath coupling operators characterize the fluctuations imposed on the system via interaction with the bosonic bath. They completely determine the impact of Gaussian fluctuations on the system under study [1]. Hence, a shift of the coupling operators  $x_j$  to  $x_j^{\text{eff}}(t)$  allows us to recover the dynamics of the system in presence of an undriven bath in thermal equilibrium. We note again, that this is only possible when the driving couples in a dipole-type manner to the individual bath oscillators. When the bath-driving would be parametric, the thermal fluctuations can be strongly altered.

### C. Redefined effective Hamiltonian

Exploiting the time-dependent shift of the position operator, we can now add Eq. (11) to the initial Hamiltonian and absorb the effective time-dependent force into both the system and system-bath coupling parts according to

$$\begin{aligned} H(t) &= H(t) - \langle H_{\text{SB}} \rangle_{\text{B}}(t) + \langle H_{\text{SB}} \rangle_{\text{B}}(t) \\ &= H_{\text{S}}^{\text{eff}}(t) + H_{\text{SB}}^{\text{eff}}(t) + H_{\text{B}}^{\text{eff}}(t) \end{aligned} \quad (16)$$

with  $H_{\text{B}}^{\text{eff}}(t)$  given in Eq. (7). As a first consequence the system-bath coupling operators are shifted, as desired,

and become time-dependent according to

$$H_{\text{SB}}^{\text{eff}}(t) = -\frac{\sigma_z}{2} \sum_j^N c_j x_j^{\text{eff}}(t) \quad (17)$$

with  $x_j^{\text{eff}}(t) = x_j - \langle \tilde{x}_j(t) \rangle_{\text{B}}^{\text{eq}}$ . In addition, the effective system Hamiltonian also becomes time-dependent as

$$H_{\text{S}}^{\text{eff}}(t) = \frac{\Delta}{2} \sigma_x + \frac{F_{\text{eff}}(t)}{2} \sigma_z. \quad (18)$$

In particular, the effective force  $F_{\text{eff}}(t)$  introduces a time-dependent asymmetry into the two-level system. This result leads to the same conclusion as drawn from earlier findings [14]. A dipole-type driving of bath modes yields an effective time-dependent force on the system. The force does not modify the fluctuational characteristics of the bath, but itself depends on its prehistory, see Eq. (13), i.e., on the full time interval  $[t_a, t]$ . In that sense, it may be denoted as a non-Markovian force.

In the following, we work with the effective Hamiltonians of Eqs. (17) and (18), but will drop the superscript ‘‘eff’’ in the symbol of the Hamiltonian from now on.

#### IV. ADIABATIC-MARKOVIAN MASTER EQUATION

Equipped with the effective Hamiltonians of Eqs. (17) and (18), we may now proceed to study the dissipative quantum dynamics. In this work, we employ a master equation approach motivated by assuming a weak system-bath coupling. In connection with the additional assumption of slow bath driving (the details are specified below), we can treat the influence of the driven bath on the basis of a Born-Markov approximation, which was previously used to investigate the dissipative Landau-Zener problem [18, 19]. A one-loop approximation of the self-energy then yields the quantum dynamics of the weakly damped and driven quantum two-level system in the form of a simple Born-Markov approximated master equation [17, 20, 27, 28]. While its derivation follows different routes, the final result coincides with the standard Born-Markov quantum master equation, see, e.g., in Ref. [7]. Similar results could also be obtained employing resummation techniques within a path-integral framework [1, 23–26].

##### A. Time-dependent rotation

As a first step, we perform a time-dependent rotation into the momentary eigenbasis of the effective system Hamiltonian (18) according to

$$\bar{H}_{\text{S}}(t) = R^\dagger(t) H_{\text{S}}(t) R(t) = \frac{E(t)}{2} \tau_x, \quad (19)$$

with the momentary eigenenergies  $E(t) = \sqrt{\Delta^2 + (F_{\text{eff}}(t))^2}$  and with  $\tau_i$  denoting the Pauli

matrices. The rotation is generated by the operator  $R(t) = \exp[i(\phi(t)/2)\sigma_y]$  with the phase  $\phi(t) = \arctan[F_{\text{eff}}(t)/\Delta]$ . Rotation of the system-bath coupling Hamiltonian yields

$$\bar{H}_{\text{SB}}(t) = -\left(\frac{u(t)}{2} \tau_z + \frac{v(t)}{2} \tau_x\right) \sum_j^N c_j x_j^{\text{eff}}(t), \quad (20)$$

with the prefactors  $u(t) = \cos \phi(t)$  and  $v(t) = \sin \phi(t)$ . For later purposes, we also define a shifted system Hamiltonian

$$\bar{H}'_{\text{S}}(t) = \bar{H}_{\text{S}}(t) + \frac{1}{2} \left(\frac{d\phi(t)}{dt}\right) \tau_y, \quad (21)$$

in which we take the time dependence of the phase into account.

##### B. Liouville space formulation

In order to evaluate the dynamics of the dissipative problem, we consider the total density matrix  $W(t)$  of the system-plus-bath at time  $t$  and make use of the Liouville-von Neumann equation of motion

$$\partial_t W(t) = -i[H(t), W(t)] \equiv \mathcal{L}(t)W(t), \quad (22)$$

with the time-dependent Liouvillian superoperator  $\mathcal{L}(t) \cdot = -i[H(t), \cdot]$  acting on operators in the product Hilbert space of system and bath. The formal solution is given by

$$W(t) = \mathcal{T} \exp \left[ \int_{t_0}^t ds \mathcal{L}(s) \right] W(t_0) = \mathcal{U}(t, t_0) W(t_0), \quad (23)$$

with the time-evolution superoperator  $\mathcal{U}(t, t_0) = \mathcal{T} \exp \left[ \int_{t_0}^t ds \mathcal{L}(s) \right]$  and  $\mathcal{T}$  denoting the proper time-ordering operator. Next, we assume complete factorization of the initial total density matrix at coupling time  $t_0$ , such that  $W(t_0) = \rho_{\text{S}}(t_0) \otimes \rho_{\text{B}}(t_0)$ . Then, we can average over the bath states to obtain the time-dependent reduced density matrix of the system

$$\rho_{\text{S}}(t) = \text{Tr}_{\text{B}} [\mathcal{U}(t, t_0) W(t_0)] = \mathcal{U}_{\text{eff}}(t, t_0) \rho_{\text{S}}(t_0). \quad (24)$$

Here, we have defined the effective time evolution superoperator  $\mathcal{U}_{\text{eff}}(t, t_0) = \text{Tr}_{\text{B}} [\mathcal{U}(t, t_0) \rho_{\text{B}}(t_0)] = \langle \mathcal{U}(t, t_0) \rangle_{\text{B}}$  of the reduced density matrix of the system. The time-evolution superoperator  $\mathcal{U}(t, t_0)$  can be expanded in a Dyson series and subsequent averaging over the bath modes then yields [27, 28] a similar expansion for the effective time-evolution superoperator

$$\begin{aligned} \mathcal{U}_{\text{eff}}(t, t_0) &= \mathcal{U}_{\text{S}}(t, t_0) + \int_{t_0}^t ds \mathcal{U}_{\text{S}}(t, s) \langle \mathcal{L}_{\text{SB}}(s) \mathcal{U}_0(s, t_0) \rangle_{\text{B}} \\ &+ \int_{t_0}^t ds \int_{t_0}^s ds' \mathcal{U}_{\text{S}}(t, s) \langle \mathcal{L}_{\text{SB}}(s) \mathcal{U}_0(s, s') \mathcal{L}_{\text{SB}}(s') \mathcal{U}(s', t_0) \rangle_{\text{B}}, \end{aligned} \quad (25)$$

where  $\mathcal{U}_0(t, t_0) = \mathcal{U}_S(t, t_0)\mathcal{U}_B(t, t_0)$  denotes the uncoupled time-evolution with  $\mathcal{U}_{S/B}(t, t_0)$  acting on the system or bath part, respectively. By combining Eqs. (24) and (25), we can recast the integral equation into the form of a master equation

$$\begin{aligned} \partial_t \rho_S(t) &= \mathcal{L}_S(t)\rho_S(t) + \langle \mathcal{L}_{SB}(t)\mathcal{U}_0(t, t_0) \rangle_B \rho_S(t_0) \\ &+ \int_{t_0}^t ds \langle \mathcal{L}_{SB}(t)\mathcal{U}_0(t, s)\mathcal{L}_{SB}(s)\mathcal{U}(s, t_0) \rangle_B \rho_S(t_0). \end{aligned} \quad (26)$$

Since the last term on the r.h.s. of this equation still contains the full superoperator  $\mathcal{U}(s, t_0)$ , it is formally exact, but needs to be approximated in order to allow for a practical solution.

### C. Adiabatic-Markovian approximation

Due to the redefined system-bath coupling in Eq. (16), the term of first order in the system-bath coupling, i.e., the second term on the r.h.s. of Eq. (26), vanishes. To see this, we note that  $\mathcal{U}_B(t, t_0)\rho_B(t_0) = \mathcal{U}_B(t, t_0)\mathcal{U}_B(t_0, t_a)\rho_B(t_a) = \mathcal{U}_B(t, t_a)\rho_B^{\text{eq}}$ , since we have defined that  $\rho_B(t_a) = \rho_B^{\text{eq}}$ . In this way, the first order term is proportional to  $\langle \tilde{x}_j^{\text{eff}}(t) \rangle_B^{\text{eq}} = 0$ .

The third term on the r.h.s. of Eq. (26) is approximated as  $\langle \mathcal{L}_{SB}(t)\mathcal{U}_0(t, s)\mathcal{L}_{SB}(s)\mathcal{U}(s, t_0) \rangle_B \approx \mathcal{M}(t, s)\mathcal{U}_{\text{eff}}(s, t_0)$  with the memory kernel  $\mathcal{M}(t, s) = \langle \mathcal{L}_{SB}(t)\mathcal{U}_0(t, s)\mathcal{L}_{SB}(s)\mathcal{U}_B(s, t_a) \rangle_B^{\text{eq}}$ . This is the Born approximation which only keeps sequential one-phonon processes in a cumulant expansion diagrammatically representing a type of one-loop approximation scheme for system-bath correlations [17, 20, 28]. We note that we explicitly kept the uncoupled driven time evolution of the bath and have used the equilibrium average pertaining to  $t_a$ . In this way, the kernel is determined by Eqs. (14) and (15) and, thus, is essentially unchanged compared to the equilibrium situation apart from the particular time dependence of  $u(t)$  and  $v(t)$ . Inserting both into Eq. (26) yields the Born-approximated quantum master equation

$$\partial_t \rho_S(t) = \tilde{\mathcal{L}}_S'(t)\rho_S(t) + \int_{t_0}^t ds \mathcal{M}(t, s)\rho_S(s), \quad (27)$$

with the memory kernel  $\mathcal{M}(t, s)$  given by

$$\mathcal{M}(t, s) = \text{Tr}_B [\tilde{\mathcal{L}}_{SB}(t)\mathcal{U}_0(t, s)\tilde{\mathcal{L}}_{SB}(s)\rho_B(s)]. \quad (28)$$

Here, we have restored the notation of the rotated Hamiltonians in Eqs. (20) and (21).

In the next step, we assume a clear separation of time scales between the dynamics associated with the system, the bath and the driving, such that the characteristic memory time  $\tau_{\text{mem}}$  of the bath is much shorter than both  $\Delta^{-1}$  and the time scale associated with the driving force. This adiabatic Markovian approximation builds on the observation that the memory kernel can then be assumed as short-lived, i.e.,  $\mathcal{M}(t-s) \ll 1$  for  $t-s \gg \tau_{\text{mem}}$ . As

such, we approximate the time evolution superoperator of the system as  $\mathcal{U}_S(t, s) \approx \exp[\tilde{\mathcal{L}}_S(t)(t-s)]$  and the time-dependent rotation parameters in  $\tilde{\mathcal{L}}_{SB}(s)$  as  $u(s) \approx u(t)$  and  $v(s) \approx v(t)$  [18, 19]. The additional time-dependence of  $\tilde{\mathcal{L}}_{SB}(s)$ , which enter via  $x_j^{\text{eff}}(t)$  in Eq. (20), is left unchanged. In this way, we preserve the time-dependent shift of the coupling operators and retain the exact equilibrium rates. Keeping this in mind, switching to the interaction picture and applying the Markov approximation [7] according to

$$\int_{t_0}^t \mathcal{M}(t, s)\rho_S(s) ds \approx \mathcal{M}_{\text{AM}}(t)\rho_S(t), \quad (29)$$

with  $\mathcal{M}_{\text{AM}}(t) = \int_{t_0}^{\infty} \mathcal{M}(t, s)e^{-\tilde{\mathcal{L}}_S(t)s} ds$ , yields a Born-Markovian quantum master equation

$$\partial_t \rho_S(t) = -i[\bar{H}'_S, \rho_S] - \Gamma(t)[\rho_S(t) - \rho_S^{\text{eq}}(t)], \quad (30)$$

that depends parametrically on time  $t$ . Here,  $\Gamma(t)$  is a momentary rate superoperator acting on both the reduced density matrix as well as the time-dependent pseudo-equilibrium statistical operator  $\rho_S^{\text{eq}}(t)$ . In the case of weak system-bath coupling, this operator becomes  $\rho_S^{\text{eq}}(t) = \frac{1}{2}[1 - r_x^{\text{eq}}(t)\tau_x]$  with  $r_x^{\text{eq}}(t) = \tanh[\beta E(t)/2]$  which is the result for a momentary thermal equilibrium. The rate coefficients in  $\Gamma(t)$  can be obtained by explicitly writing down the kernel-superoperator  $\mathcal{M}_{\text{AM}}(t)$  as a matrix in Liouville space and evaluating its elements in Laplace space [28]. Furthermore, the imaginary parts of  $\mathcal{M}_{\text{AM}}(t)$ , which give rise to frequency shifts, are neglected which is appropriate for weak system-bath coupling. The secular approximation has been invoked as well.

### D. Generalized Bloch equations

On the basis of the adiabatic Born-Markovian approximated quantum master equation (30) generalized Bloch equations can be derived as usual [7]. We find for the expectation values  $r_i(t) = -\langle \tau_i \rangle_t = -\text{Tr}[\tau_i \rho_S(t)]$  the equations of motion

$$\begin{aligned} \partial_t r_x(t) &= +\phi'(t)r_z(t) - \gamma_1(t)[r_x(t) - r_x^{\text{eq}}(t)], \\ \partial_t r_y(t) &= -\gamma_2(t)r_y(t) - E(t)r_z(t), \\ \partial_t r_z(t) &= +E(t)r_y(t) - \gamma_2(t)r_z(t) - \phi'(t)r_x(t), \end{aligned} \quad (31)$$

where the time derivative  $\phi'(t) = d\phi(t)/dt$  of the mixing angle is introduced via Eq. (21). The time-dependent rate coefficients follow as the time-dependent relaxation rate

$$\gamma_1(t) = \frac{1}{2}u^2(t)J(E(t))\coth\left(\frac{\beta E(t)}{2}\right), \quad (32)$$

and the time-dependent dephasing rate

$$\gamma_2(t) = \frac{1}{2}\gamma_1(t) + v^2(t) \left[ J(\omega)\coth\left(\frac{\beta\omega}{2}\right) \right] \Big|_{\omega \rightarrow 0}. \quad (33)$$

### E. Generalized response

To study the impact of the driven bath on the quantum two-level system, we consider the response function

$$\begin{aligned} R(t, t_0) &= \text{Tr}_S \{ i[\tilde{\sigma}_z(t, t_0), \sigma_z] \rho_S(t_0) \} \\ &= \text{Tr}_S \{ \sigma_z \mathcal{U}_{\text{eff}}(t, t_0) i[\sigma_z, \rho_S(t_0)] \}. \end{aligned} \quad (34)$$

A re-interpretation of this equation is convenient: it yields the expectation value of the operator  $\sigma_z$  weighted by the operator  $\mathcal{U}_{\text{eff}}(t, t_0) i[\sigma_z, \rho_S(t_0)]$ . In this sense, the latter operator may be identified as a different initial density matrix propagated by  $\mathcal{U}_{\text{eff}}(t, t_0)$ , whose time-dependent elements can be obtained using the Bloch equations (31). The expectation value is then provided by the linear combination  $-[u(t)r_z(t) + v(t)r_x(t)]$ . It is particularly convenient to study the frequency-dependent response function.

$$R(\omega) = \int dt e^{i\omega t} R(t, t_0). \quad (35)$$

### V. BATH DRIVING PULSES

In this work, we consider two particular bath-driving shapes: a Dirac  $\delta$ -pulse as well as a Gaussian driving-pulse. From this point onwards, we set  $t_0 = 0$  for simplicity and fix  $t_a$  and  $t_g$  separately. First, we consider a Dirac  $\delta$ -shaped driving pulse acting at  $t = t_a$  with area  $\Delta^{-1}$

$$F^\delta(t) = \Delta^{-1} \delta(t - t_a), \quad (36)$$

which generates the effective force

$$F_{\text{eff}}^\delta(t) = -\frac{1}{\Delta\pi} \int_0^\infty d\omega \bar{J}(\omega) \sin \omega(t - t_a). \quad (37)$$

As a second case, we consider a Gaussian-shaped pulse with area  $\Delta^{-1}$

$$F^g(t) = \frac{\Delta^{-1}}{\sqrt{2\pi}\sigma} e^{-\frac{(t-t_g)^2}{2\sigma^2}}, \quad (38)$$

centered at  $t = t_g$  and with a width  $\sigma$ . It generates a force

$$F_{\text{eff}}^g(t) = \text{Im} \left[ \frac{1}{2\pi\Delta} \int_0^\infty d\omega \bar{J}(\omega) e^{-\frac{\omega^2\sigma^2}{2} - i\omega(t-t_g)} \text{erfc}(\zeta_t) \right], \quad (39)$$

with  $\zeta_t = (i\omega\sigma^2 - t + t_g)/\sqrt{2\sigma^2}$  and the complementary error-function  $\text{erfc}(z)$ . For the derivation of Eq. (39), we have assumed the Gaussian at  $t_a$  to be sufficiently small and far away from the center  $t_g$ , such that the whole Gaussian is eventually taken into account during the integration in Eq. (13).

To fully characterize the effective force, we also need knowledge about the additional spectral density  $\bar{J}(\omega)$  defined in Eq. (12). As shown in Ref. [14] for two particular examples of applications, a simple proportionality

$\bar{J}(\omega) \propto J(\omega)$  can be found. This result stems from a model of a polar environmental solvent and involves linear susceptibilities for the response to emerging electrical reaction fields. Explicitly calculating the additional field-contributions from bath driving allows one to derive aforementioned proportionality. We will make use of this result here and choose the proportionality factor individually, see below. Furthermore, it should be noted that the magnitude of the force in Eqs. (36) and (38) was absorbed into the definition of  $\bar{J}(\omega)$  such that the prefactor of the latter ultimately determines the strength of the external driving.

In passing, we also note that both bath-driving pulse-shapes eventually subject the TLS to effective driving pulses of finite duration. The impact of finite pulses on the transition probability has already been investigated for pulses with various shapes [29–31]. In our case, a preliminary investigation of the excitation probability for the cases and parameters considered (not shown) leads to an oscillatory behaviour reminiscent of the  $\sin^2$ -dependence known from the Rabi-formula for rectangular pulse-shapes [29, Eq. (2)]. A detailed analysis may be subject of future works.

### VI. DYNAMICS IN A DRIVEN OHMIC BATH

First, we study the dynamical properties of the quantum two-level system in a bath with a generic Ohmic spectral density

$$J(\omega) = \frac{\eta\omega}{\omega_c} e^{-\omega/\omega_c} \quad (40)$$

with an exponential cut-off, where  $\omega_c$  is the cut-off frequency. In addition, we set  $\bar{J}(\omega) = (\bar{\eta}/\eta)J(\omega)$ . For simplicity, we evaluate the dynamics at zero temperature.

#### A. Dirac pulse

The effective force in Eq. (37) for the Dirac  $\delta$ -pulse can be obtained analytically as

$$F_{\text{eff}}^\delta(t) = -\frac{2\omega_c\bar{\eta}}{\pi\Delta} \frac{\omega_c(t-t_a)}{[1 + \omega_c^2(t-t_a)^2]^2}. \quad (41)$$

It is depicted in Fig. 2 a) for the set of parameters as indicated. In addition, the same figure shows the direct driving force  $\bar{\eta}F(t)$  for comparison. The retardation and the decay on the characteristic time scale  $1/\omega_c$  are apparent.

The ratio of the time-dependent relaxation rate of Eq. (32) and its equilibrium value is shown in Fig. 3 a). Driving leads to a visible reduction near the onset of the driving. The resulting time evolution of the components  $r_i(t) = -\langle \tau_i \rangle_t$  of the reduced density matrix are shown in Fig. 4 a). The system dynamics broadly follows the effective force profile, with the momentary population difference  $r_x(t)$  changing rapidly near the Dirac pulse. This

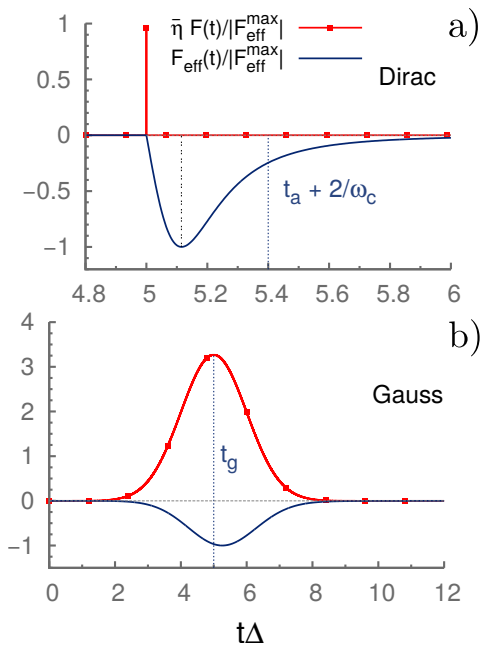


FIG. 2. Normalized effective force  $F_{\text{eff}}(t)$  (blue solid line) and direct driving force  $\bar{\eta}F(t)$  (red line with squares) for an Ohmic bath driven by a Dirac  $\delta$ -pulse (a) and a Gaussian pulse (b). The bath is characterized by the parameters  $\eta = 0.05\Delta$  and  $\omega_c = 5\Delta$ . The Dirac pulse (a) occurs at  $t_a = 5\Delta^{-1}$  with interaction strength  $\bar{\eta} = 2\Delta$ . The Gaussian pulse (b) is centered at  $t_g = 5\Delta^{-1}$  and starts at  $t_a = 0$  with interaction strength  $\bar{\eta} = 6\Delta$  and width  $\sigma = \Delta^{-1}$ . Both quantities are normalized with respect to the maximum of the effective force to allow for a comparison of relative strengths. Notice that the height of the Dirac pulse has also been chosen to correspond to its effective strength as well.

indicates an excitation of the ground state on time scales determined by the effective force. In addition, an equally abrupt emergence of coherences is also visible. For longer times, the effective force vanishes and  $r_x(t)$  decays back exponentially with a rate constant given by its equilibrium rate. However, we should keep in mind that the characteristic decay on a time scale  $1/\omega_c$  means that a comparably rapidly changing force is present. Then, the adiabatic-Markovian approximation may be problematic in this particular case.

### B. Gaussian pulse

The effective force generated by a Gaussian pulse acting on the bath, is shown in Fig. 2 b) and the resulting relaxation rate in Fig. 3 b). The dynamics of the elements  $r_i(t) = -\langle \tau_i \rangle_t$  of the reduced density matrix is shown in Fig. 4 b). The effective force follows the perturbation closely but also shows a clear retardation and fast decay as soon as the external perturbation effectively terminates. The rate and dynamics of the density matrix behave roughly in the same way as in the Dirac case, where

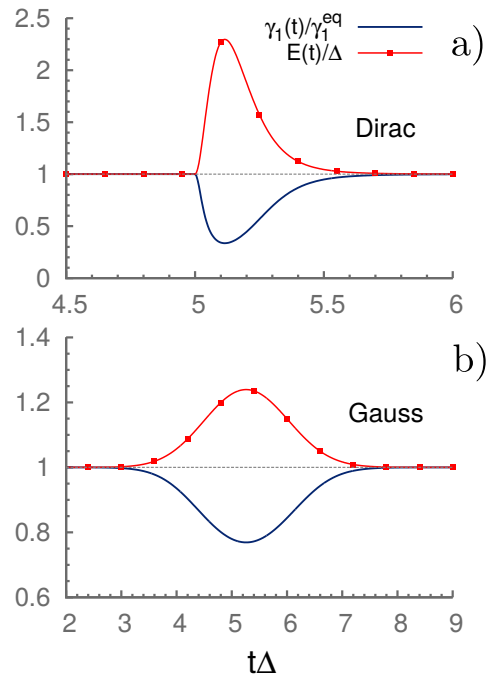


FIG. 3. Time-dependent relaxation rate (blue solid line) and momentary energy (red line with squares) for the Ohmic bath driven by a Dirac (a) and a Gaussian (b) pulse at zero temperature. The parameters are the same as in Fig. 2. The normalization has been chosen with respect to the undriven (equilibrium) relaxation rate  $\gamma_1^{\text{eq}} = J(\Delta)/2$  and the bare, undriven system energy scale  $\Delta$ .

the time-dependent rate is reduced as long as the effective force is active and the pulse leads to evident excitation of the TLS and subsequent decay with the equilibrium rate for longer times. Visible differences only occur when the Gaussian is still active. Instead of fast excitation, a plateau-like behaviour and smooth emergence of coherent superpositions can be observed. In contrast to the Dirac case, the emerging effective force is also smaller than the initial perturbation.

## VII. DYNAMICS IN A DRIVEN LORENTZIAN BATH

Another interesting class of bath spectral densities describes structured baths. A structured bath may be characterized by a Lorentzian spectral density

$$J(\omega) = \kappa \frac{\Gamma \Omega^2 \omega}{(\omega^2 - \Omega^2)^2 + (\Gamma \omega)^2}, \quad (42)$$

which has a Lorentzian peak centered at a given frequency  $\Omega$  with a width  $\Gamma$ . This additional peak may be associated with a distinct bath mode [14] and may give rise to interesting resonance effects. Instead of the structureless Ohmic spectral density of Eq. (40), the Lorentzian peak introduces a pronounced oscillatory

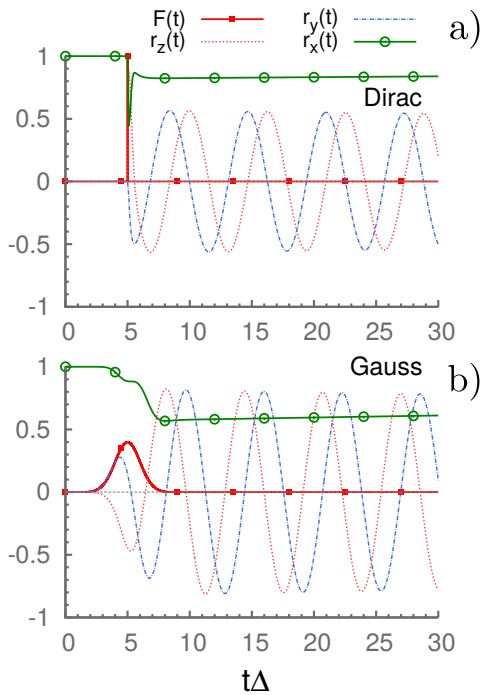


FIG. 4. Dynamics of the expectation values  $r_i(t) = -\langle \tau_i \rangle_t$  (green solid line with empty circles, dashed-dotted blue line and dotted red line) of the two-level system in an Ohmic bath at zero temperature, driven by a Dirac (a) and a Gaussian (b) pulse. The (dimensionless) external driving force  $F(t)$  is also shown (red solid line with squares) as a comparison. The dynamics are generated by the forces and rates shown in Figs. 2 and 3, with parameters being the same as in Fig. 2. The system is set to be initially in equilibrium, i.e., in the ground state.

component into the frequency response of the bath. This may be understood in terms of a convenient mapping of the Lorentzian bath onto a single harmonic oscillator with frequency  $\Omega$  which itself is coupled to a structureless Ohmic bath [21, 32]. For the case considered in this work, the coupling of the system to the single mode is given by  $g = \sqrt{\kappa\Omega/8}$  and the coupling of the mode to the Ohmic bath is given by  $h = \Gamma/(2\pi\Omega)$ . Here, we will calculate the dynamics in the original system and use aforementioned mapping for the analysis of the frequency-dependent response in section VIII. As before, we set  $\bar{J}(\omega) = (\bar{\kappa}/\kappa)J(\omega)$  and evaluate the dynamics at zero temperature.

### A. Dirac pulse

The effective driving force and the direct bath driving force for the Lorentzian bath are shown in Fig. 5 a) for a Dirac pulse. An oscillatory decay emerges which can be fitted by a function  $f(t) = -e^{-\Gamma t/2} \sin \Omega t$ , which originates from the Lorentzian peak in the spectral density. The time-dependent zero-temperature rate is shown in

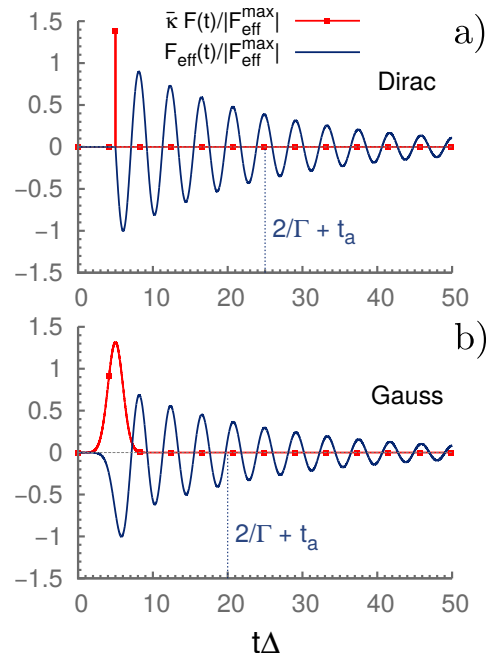


FIG. 5. Normalized effective force (blue solid line) and direct driving force  $\bar{\kappa}F(t)$  (red line with squares) for a driven Lorentzian bath with a Dirac (a) and a Gaussian (b) driving pulse. The bath is characterized by the parameters  $\kappa = 0.05\Delta$ ,  $\Omega = 1.5\Delta$  and  $\Gamma = 0.1\Delta$ . The Dirac pulse (a) occurs at  $t_a = 5\Delta^{-1}$  with interaction strength  $\bar{\kappa} = 2\Delta$ . The Gaussian pulse (b) is centered at  $t_g = 5\Delta^{-1}$  and starts at  $t_a = 0$  with interaction strength  $\bar{\kappa} = 6\Delta$  and width  $\sigma = \Delta^{-1}$ . Both quantities are normalized with respect to the maximum of the effective force to allow for a comparison of relative strengths. Notice that the height of the Dirac pulse has also been chosen to correspond to its effective strength as well.

Fig. 6 a) and behaves in a somewhat more peculiar way, with a strong alternating enhancement and suppression appearing as pronounced peaks. The rate peaks show a characteristic splitting whenever  $E(t) \geq \Omega$ . It vanishes as soon as the momentary energy becomes smaller. The splitting is a signature that enough energy for the excitation of the harmonic mode at  $\Omega$  is available which can then be used as a secondary relaxation pathway. In terms of the dynamics of the density matrix components  $r_i(t)$  shown in Fig. 7 a), the interaction with the strongly pronounced harmonic mode is visible via rapid oscillations with diverse frequency components both in the population difference as well as in the coherences. The rapid fluctuations are damped with increasing time leading to undriven exponential decay when the effective force has vanished.

### B. Gaussian pulse

The effective force generated by a Lorentzian bath driven by a Gaussian pulse is shown in Fig. 5 b). Its be-



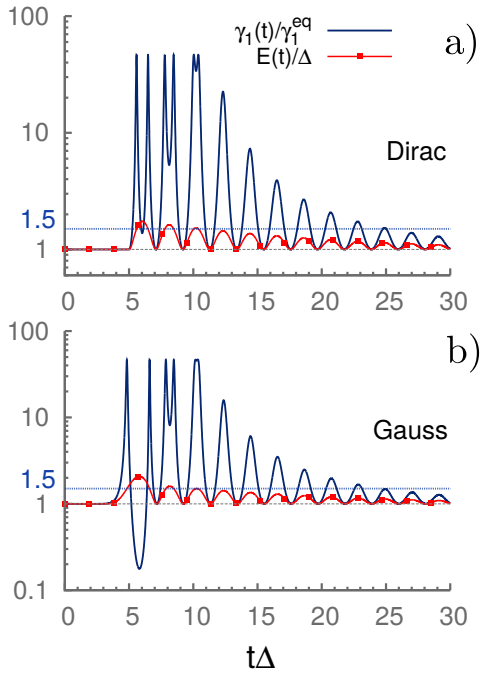


FIG. 6. Time-dependent relaxation rates (blue solid line) and momentary energy (red line with squares) for a Lorentzian bath driven by a Dirac (a) or a Gaussian (b) pulse at zero temperature. The parameters are the same as in Fig. 5. The normalization has been chosen with respect to the undriven (equilibrium) relaxation rate  $\gamma_1^{\text{eq}} = J(\Delta)/2$  and the bare, undriven system energy scale  $\Delta$ .

haviour is similar to the case of a Dirac pulse, but slight differences at short times occur due to the non-zero extent of the Gaussian pulse in time. The relaxation rate and the dynamics for the case of a Gaussian bath-driving pulse are shown in Fig. 6 b) and 7 b), respectively. Again, they show a qualitatively similar behaviour as in the previous Dirac case, with only minor differences arising when the Gaussian is still active, i.e., within a few widths of  $t_g$ .

### VIII. FREQUENCY-DEPENDENT RESPONSE

In this section, we evaluate the response function of a quantum two-level system to a driven harmonic bath. For a structureless driven Ohmic bath, it may be expected that the frequency-dependent response is only quantitatively different from the case when the bath is undriven. The situation is different for a structured Lorentzian bath, since additional resonances may be expected due to the interplay of the distinct environmental mode with the central system.

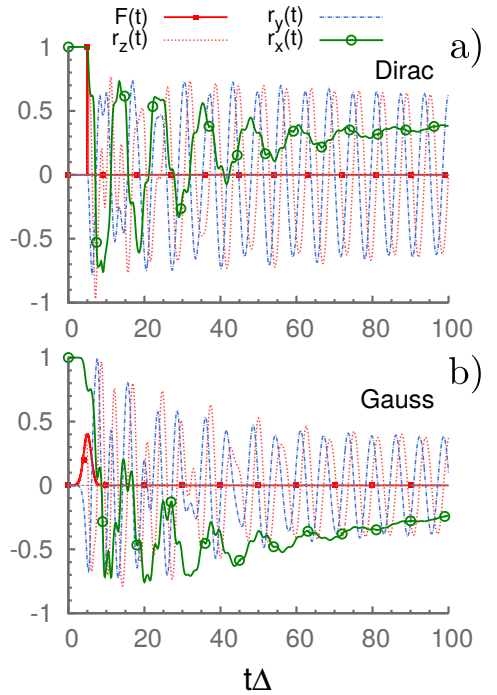


FIG. 7. Dynamics of the expectation values  $r_i(t) = -\langle \tau_i \rangle_t$  (green solid line with empty circles, dashed-dotted blue line and dotted red line) of the two-level system in a Lorentzian bath at zero temperature, driven by a Dirac (a) and a Gaussian (b) pulse. The (dimensionless) external driving force  $F(t)$  is also shown (red solid line with squares) as a comparison. The dynamics are generated by the forces and rates shown in Figs. 5 and 6, with parameters being the same as in Fig. 5. The system is set to be initially in equilibrium, i.e., in the ground state.

#### A. Driven Ohmic bath

The frequency-dependent system response of Eq. (35) for the case of a driven Ohmic bath is shown in Fig. 8 a) and b) for both driving pulse shapes in comparison to the response without bath driving. In general, Lorentzian-shaped response characteristics result, with the maximum centered at  $\omega = \Delta$ . In both cases, bath driving leads to a reduction of the central peak height, which indicates that driving of an Ohmic bath leads to less effective direct driving. For the Gaussian pulse, this effect is more pronounced, since the peak is reduced more strongly by about 30% in comparison to the undriven case.

#### B. Driven Lorentzian bath

The picture is more involved in the case of a Lorentzian bath, where the resonant interaction of the two-level system with the driven pronounced bath mode at frequency  $\Omega$  can become possible. In Fig. 8 c) and d), the frequency-dependent response close to the main frequency  $\omega \approx \Delta$

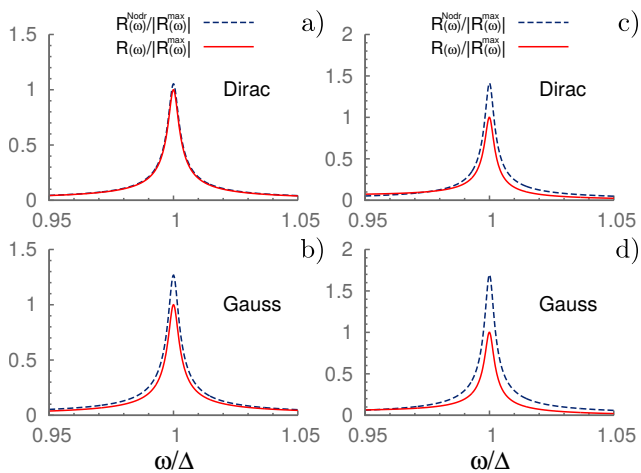


FIG. 8. Frequency-dependent response (red solid line) of a quantum two-level system to an Ohmic (a,b) and a Lorentzian (c,d) bath at zero temperature driven by a Dirac (a,c) or a Gaussian (b,d) pulse. For comparison, the response to an undriven bath is also shown (blue dashed line). The parameters used are given below Fig. 2 for the Ohmic bath and below Fig. 5 for the Lorentzian bath. Both quantities have been normalized with respect to the maximum of the driven frequency response to allow for a comparison of relative strengths.

is shown. As in the Ohmic case, the response at the main frequency is reduced when the bath-driving is included. In addition, further resonant response peaks arise which are shown in Fig. 9 a) and b). These additional resonant peaks can be understood when the mapping outlined in section VII is used. Thus, we consider the TLS coupled to a structured bath by using the equivalent situation when a TLS-plus-harmonic-oscillator is coupled to a structureless bath. The Hamiltonian of this two-level system coupled to a single harmonic oscillator with frequency  $\Omega$  and coupling strength  $g$ , is [21]

$$H_{\text{TLS-HO}} = \frac{\Delta}{2} \sigma_x - g \sigma_z (B^\dagger + B) + \Omega B^\dagger B. \quad (43)$$

Here,  $B/B^\dagger$  are the annihilation/creation operators of the harmonic oscillator. The energy level scheme of the combined TLS-plus-oscillator system is shown in Fig. 9 c) for vanishing coupling  $g$ . The corresponding transition frequencies for finite  $g$  obtained from numerical diagonalization are marked in Fig. 9 a) and b) by blue dotted lines and correspond well with the additional peaks obtained. Notable in this case is the existence of transitions from the excited TLS state (transitions 4 and 5) and both the lack of an observable shift in the two-level transition peak as well as the lack of observable level splitting between the transitions 2 and 4.

## IX. CONCLUSIONS

When an open quantum system is driven by an external time-dependent field, it is often unavoidable in prin-

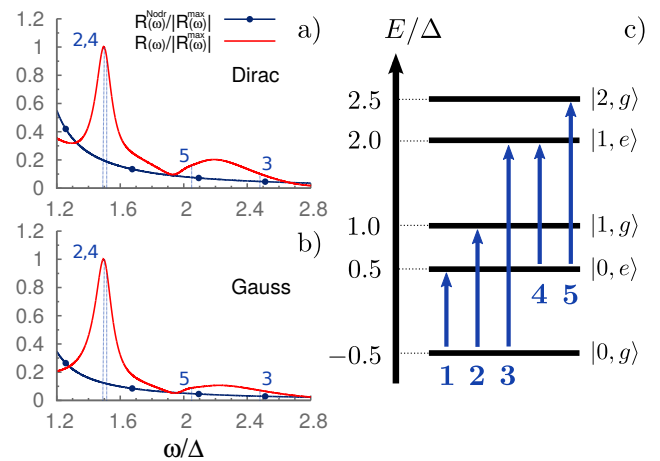


FIG. 9. Frequency-dependent response (red solid line) to a Lorentzian bath at zero temperature driven by a Dirac (a) or a Gaussian (b) pulse away from the fundamental frequency  $\Delta$ . For comparison, the response to an undriven bath is also shown (blue line with circles). The parameters used are given below Fig. 5. Both quantities have been normalized with respect to the maximum of the driven frequency response to allow for a comparison of relative strengths. The emerging peaks correspond well to energy gaps (blue dotted lines) obtained numerically from the Hamiltonian in Eq. (43) with  $g = \sqrt{\kappa}\Omega/8 \approx 0.1\Delta$  ( $\Omega = 1.5\Delta$ ). The level diagram for  $g = 0$  (c) shows the corresponding transitions (blue arrows).

ciple that the driving also couples to the environment. Usually, this effect is neglected in the theoretical description. In a sense, a special case of a driven bath is given by a pumped optical resonator in which an atom is placed. Our approach addressed a more general case by considering a continuous distribution of bath modes which can be driven.

Subsequently, we have shown that bath driving which couples linearly to the displacements of the bath oscillators (dipole-type driving) generates an additional time-dependent force for the central system. This effective force is retarded and depends on the entire time range from its onset to the momentary time as well as the spectral characteristics of the bath. We investigated this effect for the case of the spin-boson model in the weak system-bath coupling regime. In order to illustrate the emerging dynamics, we generalized a Born-Markovian quantum master equation approach in which a certain class of terms in the Liouvillian superoperator are summed up after a linearization in the system-bath coupling, while the effective force was assumed to be slow. The time-dependent bath-induced force then leads to time-dependent rate coefficients in the quantum master equation which can be solved numerically.

To be specific, we considered two types of bath spectral densities, the standard Ohmic bath and the structured Ohmic bath in which a distinct bath mode has a peaked spectral weight. Furthermore, we calculated the bath-induced force for two types of bath-driving, a

Dirac delta-shaped pulse and a Gaussian-shaped pulse. We found that the response of the central system including the bath-induced force is significantly modified. For the unstructured Ohmic bath, the resonant response of the quantum two-level system is effectively reduced when bath driving is included. Interestingly enough, a qualitatively different response arises when a structured Ohmic bath with a Lorentzian peak in the environmental spectral density is considered. Then, additional resonant peaks appear in the response of the system when the external drive excites the pronounced bath mode.

Since driven dissipative quantum systems are ubiquitous, the effect described in the present work should be

considered in an accurate theoretical description of the time-dependent response and may provide a basis for new, elaborate driving schemes.

## ACKNOWLEDGMENTS

We acknowledge financial support of “The Hamburg Centre for Ultrafast Imaging (CUI)” within the German Excellence Initiative supported by the Deutsche Forschungsgemeinschaft.

- 
- [1] U. Weiss, *Quantum Dissipative Systems*, 4th ed. (World Scientific, Singapore, 2012).
  - [2] A. J. Leggett, S. Chakravarty, A.T. Dorsey, M.P.A. Fisher, A. Garg, and W. Zwerger, *Rev. Mod. Phys.* **59**,1 (1987); **67**, 725 (E) (1995).
  - [3] W. A. Phillips, *Rep. Prog. Phys.* **50**, 1657 (1987).
  - [4] P. Nalbach, D. Osheroff and S. Ludwig, *J. Low Temp. Phys.* **137**, 395 (2004).
  - [5] C. Enss and S. Hunklinger, *Low Temperature Physics* (Springer-Verlag, Berlin, 2005).
  - [6] A. J. Leggett and D. C. Vural, *J. Phys. Chem. B* **117**, 12966 (2013).
  - [7] A. Nitzan, *Chemical Dynamics in Condensed Phases*, (Oxford Univ. Press, Oxford, 2006).
  - [8] H. van Amerongen, L. Valkunas, and R. van Grondelle, *Photosynthetic Excitons* (World Scientific, Singapore, 2000).
  - [9] R. Hanson, L. P. Kouwenhoven, J. R. Petta, S. Tarucha, and L. M. K. Vandersypen, *Rev. Mod. Phys.* **79**, 1217 (2007).
  - [10] Y. Makhlin, G. Schoen, and A. Shnirman, *Rev. Mod. Phys.* **73**, 357 (2001).
  - [11] M. Grifoni and P. Hänggi, *Phys. Rep.* **304**, 229 (1998).
  - [12] M. Thorwart, M. Grifoni and P. Hänggi, *Phys. Rev. Lett.* **85**, 860 (2000).
  - [13] M. Thorwart, M. Grifoni and P. Hänggi, *Ann. Phys. (N.Y.)* **293**, 15 (2001).
  - [14] H. Grabert, P. Nalbach, J. Reichert and M. Thorwart, *J. Phys. Chem. Lett.* **7**, 2015 (2016).
  - [15] H. Grabert, *Phys. Rev. B* **92**, 245433 (2015).
  - [16] M. Frey and H. Grabert, *Phys. Rev. B* **94**, 045429 (2016).
  - [17] A. Würger, *J. Phys.: Condens. Matter* **9**, 5543 (1997).
  - [18] P. Nalbach, J. Knörzer and S. Ludwig, *Phys. Rev. B* **87**, 165425 (2013).
  - [19] P. Nalbach, *Phys. Rev. A* **90**, 042112 (2014).
  - [20] P. Nalbach, Ph.D. thesis, Ruprecht-Karls Universität Heidelberg, 1999
  - [21] M. Thorwart, E. Paladino and M. Grifoni, *Chem. Phys.* **296**, 333 (2004).
  - [22] E. Merzbacher, *Quantum Mechanics*, 3rd ed. (Wiley, Hoboken, NJ, 1998).
  - [23] U. Weiss and M. Wollensak, *Phys. Rev. Lett.* **62**, 1663 (1989).
  - [24] R. Görlich, M. Sassetti, and U. Weiss, *Europhys. Lett.* **10**, 507 (1989).
  - [25] M. Grifoni, M. Sassetti, and U. Weiss, *Phys. Rev. E* **53**, R2033 (1996).
  - [26] M. Grifoni, M. Winterstetter, and U. Weiss, *Phys. Rev. E* **56**, 334 (1997).
  - [27] P. Nalbach *Phys. Rev. B* **66**, 134107 (2002)
  - [28] P. Nalbach and M. Thorwart, *J. Chem. Phys.* **132**, 194111 (2010).
  - [29] I. I. Boradjiev and N. V. Vitanov, *Phys. Rev. A* **88**, 013402 (2013).
  - [30] G. S. Vasilev and N. V. Vitanov, *Phys. Rev. A* **70**, 053407 (2004).
  - [31] C. W. S. Conover, *Phys. Rev. A* **84**, 063416 (2011).
  - [32] A. Garg, J.N. Onuchic and V. Ambegaokar, *J. Chem. Phys.* **83**, 4491 (1985).